Millimeter-Wave Amplitude-Phase Modulator

Alexander E. Martynyuk, Ninel A. Martynyuk, Sergei N. Khotiaintsev, *Senior Member, IEEE,* and Valeri S. Vountesmeri

***Abstract*— A millimeter-wave amplitude-phase modulator, using Fox's (polarization) principle of phase changing has been developed. Using this modulator, it is possible to perform the following types of phase modulation: binary phase-shift keying (BPSK), quadrature phase-shift keying (QPSK), differential QPSK (DQPSK), $\pi/4$-DQPSK with peak phase error 5° (rms error: 2°), and peak amplitude error 2% (rms error: 1%) in the frequency range of 36–37.5 GHz. The achievable switching time is less than 35 ns. A low level of insertion loss (1 dB) is achieved. The modulator is able to switch up to 25 dBm of RF power. This modulator can also be used for changing the amplitude of the output wave from 0 to −6 dB with an accompanying phase modulation less than 3°. The modulator is suitable for use in high-speed millimeter-wave communication systems.**

***Index Terms*— Millimeter-wave modulation, millimeter-wave phase shifter, millimeter-wave radio communication, phase modulation, phase-shift keying.**

I. Introduction

MILLIMETER-WAVE communication systems are very helpful for both military and commercial applications [1], [2]. For terrestrial telecommunications, the trend is to increase the spectral efficiency, so complex modulation methods are used [3], [4]. At the present time, modulation of low frequencies with upconversion, and then power amplification, is the most commonly used method in microwave communication systems. However, it is very difficult to realize this approach with millimeter waves due to the absence of effective and low-cost power amplifiers. Therefore, direct modulation with the help of an amplitude-phase modulator may be used as an alternative approach for millimeter waves [5]; however, in this case, very strict limitations exist for phase errors and the insertion loss level. To satisfy these heavy requirements, the authors are using Fox's [7] principle of phase changing. This method has the advantage of low phase errors and a low level of the accompanying amplitude modulation and was successfully applied for developing a spiraphase-type phased array [6]. This paper describes the amplitude-phase modulator, which is suitable for use in high-speed communication systems in the 36–37.5-GHz frequency range due to extremely small phase errors, a relatively low level of the insertion loss, and fast operation. Design considerations are presented and experimental characteristics of the fabricated modulator are discussed. It is demonstrated that it is possible to change the amplitude of the output signal in the range from 0 to −6 dB without changing the phase.

Manuscript received March 19, 1996; revised February 28, 1997.

A. E. Martynyuk was with the Theoretical Radio Engineering Department, Kiev Polytechnic Institute, Kiev, Ukraine. He is now with Centro de Instrumentos, Universidad Nacional Autonoma de Mexico, Cd Universitaria A.P. 70-186, C.P. 04510, Mexico.

N. A. Martynyuk was with Programa Universitario de Investigacion y Desarrollo Espacial, Universidad Nacional Autonoma de Mexico, Mexico. She is now with the Theoretical Radio Engineering Department, Kiev Polytechnic Institute, Kiev, Ukraine.

S. N. Khotiaintsev is with the Microwave and Laser Laboratory, Institute of Physiology, Puebla University, Puebla, Mexico.

V. S. Vountesmeri is with Centro de Instrumentos, Universidad Nacional Autonoma de Mexico, Cd Universitaria A.P. 70-186, C.P. 04510, Mexico.

Publisher Item Identifier S 0018-9480(97)03913-6.

II. Basic Considerations

The basic construction of the amplitude-phase modulator is shown in Fig. 1. It consists of the following elements:

- circulator A;
- rectangular-to-circular waveguide transition B for transformation of TE_{10} mode of rectangular waveguide to y-polarized TE_{11} mode of circular waveguide;
- polarization filter C, consisting of two printed $\lambda/2$-length horizontal dipoles, situated $\lambda/4$ from one another; one dipole is terminated in a short circuit, the other is loaded on the matched resistor, therefore, x-polarized wave, traveling in negative $\vec{z}$ direction is dissipated;
- polarizer D-differential 90° section, for transforming y-polarized mode TE_{11} to the circularly-polarized mode TE_{11} of circular waveguide;
- control section E, consisting of section of circular waveguide terminated in short circuit with control diaphragm in its cross section.

Let's consider the mode TE_{10} at the input of the modulator (Fig. 1). After traveling through the circulator, the rectangular–to–circular waveguide transition and the polarization filter, the mode TE_{10} transforms to the vertically polarized mode TE_{11} of the circular waveguide. This vertically polarized mode is transformed to the circularly polarized mode TE_{11} with the help of a polarizer. Then the incident circularly polarized mode TE_{11} is reflected by the control section. The control section is built in such a way that the reflected wave may be considered as a sum of two circularly polarized waves. One of these waves is a circularly polarized wave where the electric-field vector rotates in the same direction as the electric-field vector of the incident wave. The phase and amplitude of this wave are controlled by the control section. The second reflected component is the wave where the electric-field vector rotates in the opposite direction. Only the amplitude of this component is controlled by the control section. The first component shall be called the *controlled wave*, and meanwhile the second component shall be called the *uncontrolled wave*.

The reflected controlled and uncontrolled waves are transformed by the polarizer to vertically and horizontally polarized

0018–9480/97$10.00 © 1997 IEEE

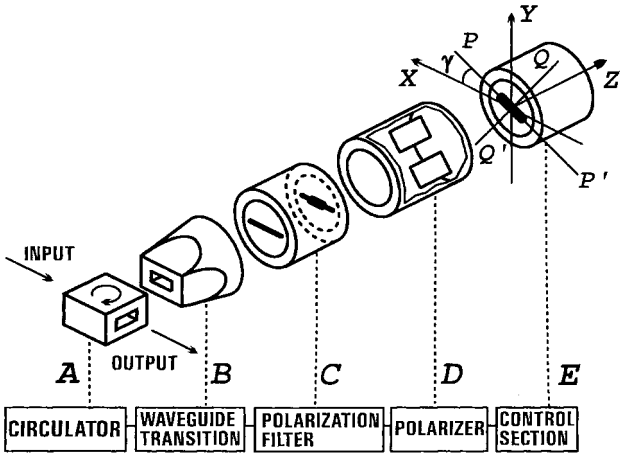

Fig. 1. The basic construction of the amplitude-phase modulator.

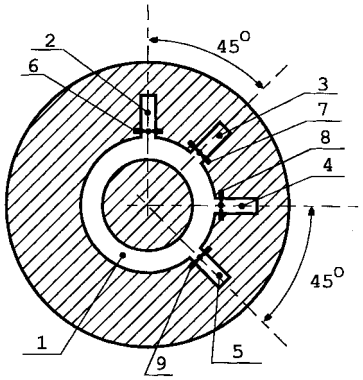

Fig. 2. The control diaphragm of the amplitude-phase modulator with four possible phase conditions.

waves, respectively. Then the horizontally polarized wave is dissipated in the polarization filter, but the controlled wave is transformed to mode TE_{10} of the rectangular waveguide. Then the circulator is used to separate the incident wave from the reflected one.

The control section uses Fox's principle of phase changing. One can consider the control section as a section of a circular waveguide terminated in a short circuit with the control diaphragm in its cross section. The control section provides different reflection coefficients $\Gamma_\perp$ and $\Gamma_\parallel$ for two orthogonal linearly polarized modes with vectors of electric-field density $\vec{E}$ parallel to the axes PP' and QQ', respectively. Let one assume that a circularly polarized incident wave propagates toward the control section as follows:

$$\vec{E}_i = E_0(\vec{e}_x + j\vec{e}_y)e^{-j\beta z} \tag{1}$$

where E_0 is the amplitude of the incident wave, $\vec{e}_x$ and $\vec{e}_y$ are the unit vectors in the $\vec{x}$ and $\vec{y}$ directions, and $j = \sqrt{-1}$.

The reflected wave can be expressed as a sum of the circularly polarized waves

$$\begin{aligned}\vec{E}_r =& 0.5E_0e^{2j\gamma}(\Gamma_\parallel - \Gamma_\perp)(\vec{e}_x - j\vec{e}_y)e^{j\beta z} \\ &+ 0.5E_0(\Gamma_\parallel + \Gamma_\perp)(\vec{e}_x + j\vec{e}_y)e^{j\beta z}\end{aligned} \tag{2}$$

where γ is the angle between the axis $\vec{x}$ and the axis PP'.

The first component of the sum (2) is a circularly polarized wave with the same direction of rotation as vector $\vec{E}_i$, which is the incident wave. One can control the phase of this wave by changing angle γ. The second component of the sum is the wave with the opposite direction of rotation as vector $\vec{E}_i$. The phase of this component is not changed by changing angle γ. The amplitude of the controlled wave is at its maximum when

$$\Gamma_\perp = -\Gamma_\parallel = \Gamma_{\text{opt}}. \tag{3}$$

In this case, the amplitude of the uncontrolled wave, the second component of (2), is equal to zero and the modulator has minimal possible loss, which is determined only by the quality of the switching elements used. Therefore, it is necessary to provide an additional differential 180° phase shift between orthogonal components of the reflected wave. If values $\Gamma_\perp$ and $\Gamma_\parallel$ do not change while changing the angle γ, only the phase changes in the reflected wave.

If one changes the absolute value of $\Gamma_\perp$ from Γ_{opt} to zero, the amplitude of the controlled wave will reduce twice, but the phase of the controlled wave does not change its value. With the help of this method, one can control the amplitude of the reflected wave. At least when $\Gamma_\perp = \Gamma_\parallel$, one can reduce the amplitude of the controlled wave to zero.

Therefore, the phase of the controlled wave is determined only by the angle γ, while the amplitude of the controlled wave can take values between 0 and -6 dB.

III. Control Section Design

In the simplest case, the control section can be realized as a thin $\lambda/2$-dipole terminated in a short circuit, installed in the cross section of the $\lambda/4$-section of the circular waveguide terminated in a short circuit. The $\lambda/2$-dipole terminated in a short circuit reflects a linearly polarized mode TE_{11} with vector $\vec{E}$ parallel to the dipole and has no influence on the mode TE_{11} with orthogonal polarization. Therefore, an additional differential phase shift of 180° appears between orthogonal components of the reflected wave. By rotating the dipole, one can control the phase of the reflected wave. In this case, the velocity of the phase change is not sufficient for communication applications, so it is necessary to use an electronic simulation of the mechanical rotation. One can obtain this simulation by using switching p-i-n diodes, which are situated on the surface of the control diaphragm.

The control diaphragm for the modulator with the four possible phase conditions is shown in Fig. 2. The control diaphragm is the system of connected slot resonators, which consist of a ring slot 1 with an average diameter $\frac{\lambda}{\pi}$ (the average length of the slot is λ) and inductive radial stubs 2–5. These stubs are connected to the ring slot in series and the angle between the nearest stubs is 45°. The switching diodes 6–9 are connected in parallel to the inductive stubs. At any time, three diodes are switched on and one diode is switched off.

When diode 6 is switched off, the linearly polarized component of the incident circularly polarized wave with vector $\vec{E}$, which is parallel to stub 2's axis of symmetry does not excite significant fields in stubs 3–5 because these stubs are shorted by switched-on diodes and the length of each stub

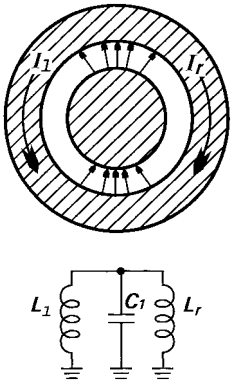

Fig. 3. The ring slot resonator and its equivalent circuit.

is less then $\lambda/4$. Excited fields of stub 2 are negligible also, due to the symmetry of the incident field and the diaphragm's configuration. Therefore, the control diaphragm for the linearly polarized component mentioned above is equivalent to the ring slot resonator and all the fields excited on the surface of the control diaphragm have the same dependence on the angular variable as the incident linearly polarized component. As a result, one has different values of the high-frequency (HF) currents that flow across the switched-on diodes. These values depend upon the angular location of each diode and are proportional to $\sin\theta$, where θ is the angle between the electric-field vector of the exciting wave and the stub's axis of symmetry, and is also the angle which determines the angular location of each diode.

When the frequency of the exciting field is equal to the resonant frequency of the ring slot resonator, mode TE_{11} can pass through the control diaphragm without reflection. The no-load condition in the plane of the diaphragm for this linearly polarized component of the incident circularly polarized wave is obtained by placing a metal wall at a distance of $\lambda/4$ from the control diaphragm.

In order to determine the level of the insertion loss for this case, one needs to build an appropriate model. The rigorous solution of the integral equation for the presented structure is available but quite complex, which makes its use in the optimization process very difficult. Therefore, a simple model is used based on the fact that the mentioned structure is similar to the ring slot resonator. The geometry of the ring slot resonator and its equivalent circuit are illustrated in Fig. 3. In the ring slot resonator, the magnetic energy is stored mainly due to the electric currents I_r and I_l, which flow across the right and left part of the outer conductive ring, respectively. The electric energy is stored due to the concentration of the electric field in the ring slot. The equivalent circuit used is a parallel resonant circuit with the resonant frequency $\omega_{or} = \sqrt{(2/L_r C_1)}$. It contains two equal inductances L_l, L_r and capacitance C_1. Now one needs to modify the presented circuit in order to take into account the switching elements and the inductive stubs. Since only the right side of the ring slot resonator was changed (Fig. 2), the appropriate changes were made in the equivalent circuit. The modified equivalent circuit is presented in Fig. 4(a), where L_s is the inductance of the stub terminated in a short circuit and r_d, L_d are the resistance of

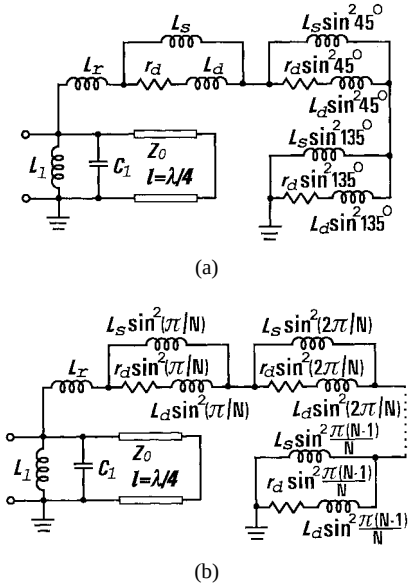

Fig. 4. The equivalent circuit of the control section of the amplitude-phase modulator with (a) four possible phase conditions and (b) N possible phase conditions (for the scattering of the linearly polarized mode TE_{11} with vector $\vec{E}$ parallel to the axis of symmetry of the stub, where the switched-off diode is situated).

the switched-on p-i-n diode and the inductance of the diode's leads, respectively. The RF power dissipated in a switched-on diode is proportional to $\sin^2\theta$, while the equal RF current flows across the circuits, which are equivalent to the switched-on diodes [see Fig. 4(a)]. Therefore, the multiplication of the diode's and stub's impedance by trigonometric function $\sin^2\theta$ is used in order to conserve power relations. The transmission line terminated in a short circuit with characteristic impedance Z_0 and length $\lambda/4$ is equivalent to the $\lambda/4$-section of the circular waveguide terminated in the short circuit. For this case, the equivalent resistance of the control diaphragm at the resonant frequency $\omega_{04} = \sqrt{2(L_r + L_d)/(L_l C_1(L_r + 2L_d))}$ can be determined according to the following equation (assume that the impedance of the switched-on diode is small compared to the input impedance of the stub terminated in a short circuit):

$$R_{e4} = \frac{[\omega_{04}(L_r + 2L_d)]^2}{2r_d}. \tag{4}$$

The control diaphragm for the modulator with N possible phase conditions has N radial inductive stubs, with the angle between the two nearest stubs being $180°/N$. In this case, one has $N-1$ switched-on diodes and one switched-off diode on the surface of the control diaphragm. The equivalent circuit for the control diaphragm of the modulator with N possible phase conditions ($N = 2^m, m = 1, 2, 3, \cdots$) is shown in Fig. 4(b). The equivalent resistance of the control diaphragm at the resonant frequency can be evaluated as follows (the same simplification is assumed and the relation $\sum_{n=1}^{N} \sin^2\left(\frac{n\pi}{N}\right) = \frac{N}{2}$ is used):

$$R_{eN} = \frac{2[\omega_{0N}(L_r + NL_d/2)]^2}{Nr_d} \tag{5}$$

where ω_{0N} is the resonant frequency of the control diaphragm.

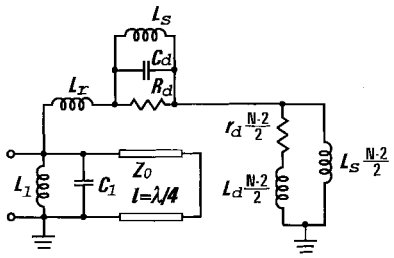

Fig. 5. The equivalent circuit of the control section of the amplitude-phase modulator with possible phase conditions (for the scattering of the linearly polarized mode TE_{11} with vector $\vec{E}$ orthogonal to the axis of symmetry of the stub, where the switched-off diode is situated).

Therefore, at the resonant frequency, the reflection coefficient from the control section can be written as follows (assuming that $R_{en} \gg Z_0$):

$$\Gamma_\perp = \frac{R_{eN} - Z_0}{R_{eN} + Z_0} \approx 1 - \frac{2Z_0}{R_{eN}}. \tag{6}$$

One then substitutes R_{eN} of (5) into that of (6) to obtain

$$\Gamma_\perp = 1 - \frac{NZ_0 r_d}{[\omega_{0N}(L_r + NL_d/2)]^2}, \tag{7}$$

Now, assume scattering of the linearly polarized component of the incident circularly polarized wave, in which vector $\vec{E}$ is orthogonal to the axis of symmetry of stub 2, where the switched-off diode 6 is situated (Fig. 2). Stub 2 is excited by the wave of this polarization. The equivalent circuit of the control diaphragm of the N-discrete modulator for this case is shown in Fig. 5 (the relation $\sum_{n=1}^{N} \sin^2\left(\frac{n\pi}{N}\right) = \frac{N}{2}$ was used to simplify the circuit). The length of each stub was chosen to obtain the series resonance of the control diaphragm with the same resonant frequency as for the parallel resonant circuit in the case mentioned above. The series resonant circuit contains inductance $L_r + L_d(N/2-1)$ with reactance X_L and the parallel connection of two reactive elements C_d, L_s with reactance $-X_L$ (where C_d and R_d are the capacitance and parallel resistance of the switched-off diode, respectively). Therefore, the equivalent impedance of the control diaphragm is a small active resistance at the resonant frequency. The incident wave of this polarization is reflected by the diaphragm with a reflection coefficient that is approximately -1, hence, an additional differential phase shift of 180° is provided between orthogonal linearly polarized components of the reflected wave. By switching the diodes one can simulate the mechanical rotation of the control diaphragm, so one now has an additional phase shift in the reflected circularly polarized wave.

It is possible to calculate an equivalent resistance of the control diaphragm in the case of the series resonance according to the following formula (assuming that the inductive impedance of the diode's leads is small compared to the reactive impedance of the switched-off diode and that the resistance of the switched-off diode is large compared to its reactive impedance):

$$r_{eN} = \left(\frac{N}{2} - 1\right) r_d + \frac{[\omega_{0N}(L_r + (N/2-1)L_d)]^2}{R_d}. \tag{8}$$

Hence, at the resonant frequency ω_{0N}, the reflection coefficient can be expressed as shown in (9) at the bottom of the page (assume that $r_{eN} \ll Z_0$). Minimal insertion loss and rejection of the uncontrolled wave occurs when absolute values of $\Gamma_\perp$ and $\Gamma_{||}$ are equal. Therefore, using formulas (7) and (9), it is possible to obtain an equation for the control diaphragm's equivalent circuit optimization

$$\frac{(N-2)r_d}{Z_0} + \frac{2X_L^2}{Z_0 R_d} = \frac{NZ_0 r_d}{X_L^2} \tag{10}$$

where $X_L = \omega_{0N}(L_r + L_d N/2) \approx \omega_{0N}(L_r + L_d(N/2-1))$, since the lead's inductance is relatively small.

By resolving (10) with respect to X_L, it is possible to formulate an equation for obtaining optimal X_L^2

$$X_{L\text{opt}}^2 = \frac{-(N-2)r_d R_d + \sqrt{(N-2)^2 r_d^2 R_d^2 + 8NZ_0^2 r_d R_d}}{4}. \tag{11}$$

If one uses p-i-n diodes with typical values of r_d 2–6 Ω, R_d 5–15 kΩ, and for $N \leq 16$, one can simplify (11) by ignoring the first component under the root and the first term of the numerator. These simplifications are equivalent to ignoring the second term of (9), hence, one assumes that a decrease in the absolute value of $\Gamma_{||}$ occurs only due to the finite value of R_d and half of the dissipated millimeter-wave power is dissipated in the switched-off diode. Therefore, one has

$$X_{L\text{opt}}^2 = (\omega_{oN}(L_r + NL_d/2))^2 = Z_0\sqrt{Nr_d R_d/2}. \tag{12}$$

The value of X_L^2 is determined mainly by the parameters of the ring slot resonator. Construction of the control diaphragm permits one to obtain different values of X_L. The resonant frequency of the ring slot resonator is determined only by the average length of the ring, but one can change the quality factor of the ring slot resonator (or X_L) by changing the width of the slot. It is possible to increase the value of X_L by increasing the width of the slot resonator. Decreasing the slot's width leads to a decrease in the value of X_L. Hence, one has the possibility of changing the value of X_L to obtain the optimal value. By substituting (12) into (7), one is able to obtain the value of Γ_{opt} as follows:

$$\Gamma_{\text{opt}} = 1 - \sqrt{\frac{2Nr_d}{R_d}}. \tag{13}$$

Therefore, one can now find the formula for the insertion loss in the optimized modulator with N possible phase

$$\Gamma_{||} = \frac{r_{eN} - Z_0}{r_{eN} + Z_0} \approx -1 + \frac{2r_{eN}}{Z_0} = -1 + \frac{(N-2)r_d}{Z_0} + \frac{2[\omega_{0N}(L_r + (N/2-1)L_d)]^2}{Z_0 R_d} \tag{9}$$

conditions

$$L_{\rm opt} = 10\log{\Gamma_{\rm opt}}^2 \approx 10\log\left(1 - 2\sqrt{\frac{2Nr_d}{R_d}}\right). \quad (14)$$

The insertion loss is determined only by the parameters of the switching elements and the number of the possible phase conditions N.

Since many system applications require a significant level of millimeter-wave power, it is desirable to obtain closed-form expressions for the maximum level of the input power. Excessive input RF power causes permanent damage of the p-i-n diodes or damage of the thin-film resistor in the polarization filter. Assume that the optimized amplitude-phase modulator operates in the pure phase modulation mode with the minimum possible level of the insertion loss. In this case, one can consider that the power dissipated in the thin-film resistor is negligible. Therefore, the RF power that can be handled safely by the modulator is limited by two factors: the breakdown voltage of the switched-off diode $V_{\max}$ and the thermal considerations (or maximum power dissipation in the p-i-n diode $P_{\max}$). According to previous analysis, the switched-off diode operates in the heaviest conditions, dissipating half of the total dissipated millimeter-wave power. Using formula (13), one can evaluate the level of RF power dissipated by the switched-off diode

$$P_{\rm off} = 0.5\left(1 - {\Gamma_{\rm opt}}^2\right)P_{\rm in} \le P_{\max} \quad (15)$$

where $P_{\rm in}$ is the input millimeter-wave power.

Now one can obtain one of the two maximum power level limitations

$$P_{\rm in} \le \sqrt{\frac{R_d}{2Nr_d}}P_{\max} = P'_{\rm inmax}. \quad (16)$$

The second maximum power-level limitation one can obtain by substituting in (16) $P_{\max} = V_{\max}^2/(8R_d)$ is as follows:

$$P_{\rm in} \le \frac{1}{8}\sqrt{\frac{1}{2NR_dr_d}}V_{\max}^2 = P''_{\rm inmax}. \quad (17)$$

Now consider the operation of the amplitude-phase modulator with amplitude modulation under the assumption that each p-i-n diode operates as a linear resistor even with small forward bias currents. In this case, the heaviest situation exists when -6 dB of attenuation is obtained and half of the input power is dissipated in the switched-on diodes. Power, dissipated in the diode which operates under the heaviest conditions, may be evaluated in accordance with the formula

$$P_{\rm in6dB} = \frac{P_{\rm in}}{N} \le P_{\max}. \quad (18)$$

Now one can obtain the third limitation for the input power

$$P_{\rm in} \le NP_{\max} = P'''_{\rm inmax}. \quad (19)$$

Calculated values of $P'_{\rm inmax}$, $P''_{\rm inmax}$, and $P'''_{\rm inmax}$ are shown in Table I. The calculations were made for the following parameters of the diode: $P_{\max} = 250$ mW, $V_{\max} = 100$ V, $r_d = 3\ \Omega, R_d = 10$ k$\Omega, T_d = 25$ °C.

TABLE I
THE MINIMAL LEVEL OF INSERTION LOSS AND THE MAXIMUM POWER LEVELS FOR THE N-DISCRETE MODULATOR

	N=4	N=8	N=16
L_{opt},dB	-0.45	-0.65	-0.95
$P'_{in\ max}$,W	5.10	3.61	2.55
$P''_{in\ max}$,W	2.55	1.80	1.28
$P'''_{in\ max}$,W	1	2	4

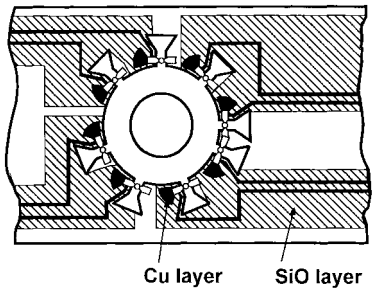

Fig. 6. The control diaphragm of the amplitude-phase modulator with eight possible phase conditions.

IV. MODULATOR DESIGN AND PERFORMANCE

A. Circuit Description

The final construction of the control diaphragm of the modulator with eight possible phase conditions (0°, 45°, 90°, 135°, 180°, 225°, 270°, 315°) is shown in Fig. 6. Inductive stubs are situated uniformly over the ring slot resonator to obtain approximate symmetry of the control diaphragm. The form of the stub chosen was trapezoidal to reduce the length of the stubs. All bias circuits and switching diodes were situated on the surface of the thick (0.4-mm) copper plate. Special attention was paid to the reduction of the insertion loss in the bias circuits. Bias circuits and metal–dielectric–metal filters for the separation of RF and dc currents were fabricated on the copper plate using special thin-film technology, proposed by Skachko. A thin (5 μm) SiO_2 layer was used as a high-quality dielectric. The inner part of the ring slot resonator was made on glass microfiber reinforced polytetrafluorethylene (PTFE) material with a dielectric constant of 2.5 and a thickness of dielectric of 60 μm. This inner part was connected to the main copper plate by soldering. The radius of the circular waveguide was 3.6 mm and the dimensions of the inner and outer radius of the ring slot resonator were obtained by applying the optimization process described above.

Diaphragms of the polarization filter were fabricated on the microfiber reinforced PTFE material, the width of the dipoles was 400 μm, and the value of the matched thin-film chromium resistor was 215 Ω. The rectangular-to-circular waveguide transition was a stepped transition with length 10.5 mm and standing-wave ratio (SWR) less then 1.07 in the 36–37.5-GHz frequency range. The polarizer was a differential 90° section of a finned circular waveguide with length 15 mm, and SWR less then 1.1 in the 36–37.5-GHz frequency range.

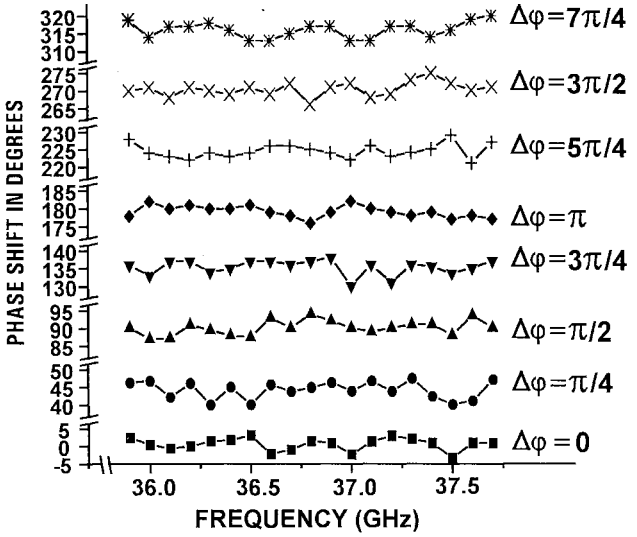

Fig. 7. Measured phase shift of the amplitude-phase modulator for the minimal level of insertion loss.

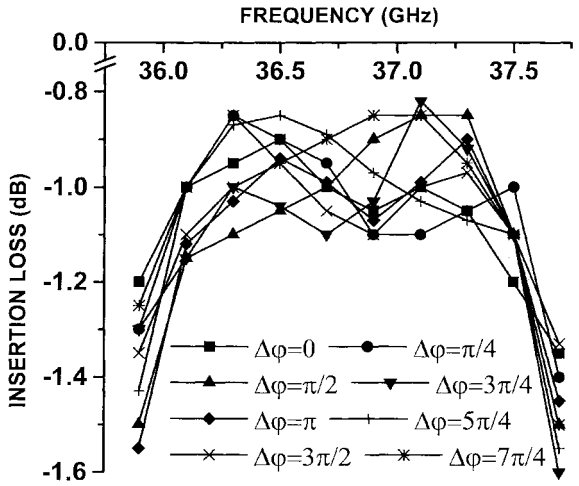

Fig. 8. Measured insertion loss of the amplitude-phase modulator (the circulator's insertion loss is excluded).

B. Experimental Results

The measured results are depicted in Figs. 7 and 8. The phase shift for the eight possible phase conditions of the modulator is given in Fig. 7. In the 36–37.5-GHz frequency range, peak phase errors are less than 5° for all eight phase conditions of the modulator. Measured insertion loss is presented in Fig. 8 (the circulator's insertion loss is excluded). An insertion loss of 1±0.15 dB was obtained for all possible phase conditions of the amplitude-phase modulator in the 36–37.5-GHz frequency range, therefore, amplitude imbalance between two arbitrarily chosen phase conditions is less than 0.3 dB. The insertion loss is quite near to the predicted level (Table I), so insertion loss in the bias circuits is negligible. Switching time less than 35 ns was achieved, the modulator was able to switch at least 400 mW of RF power without any significant change of performance.

A possibility for independent changing of the amplitude was investigated. For a reduction of the amplitude of the reflected wave, forward currents of all switched-on diodes were reduced simultaneously. Fig. 9 shows an increase of insertion loss while the diode's direct current is decreasing. This change of the amplitude does not cause significant phase changing in the reflected wave (see Fig. 10). Finally, more then 23-dB isolation was obtained in the 36–37-GHz frequency range when the forward bias current was applied across all eight diodes.

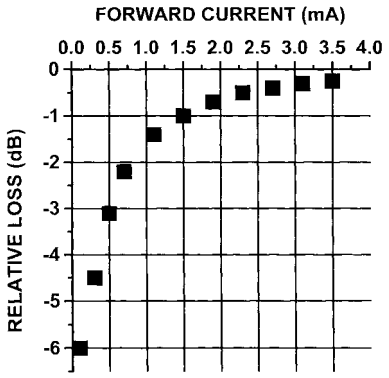

Fig. 9. Measured relative insertion loss of the amplitude-phase modulator as a function of the forward bias current.

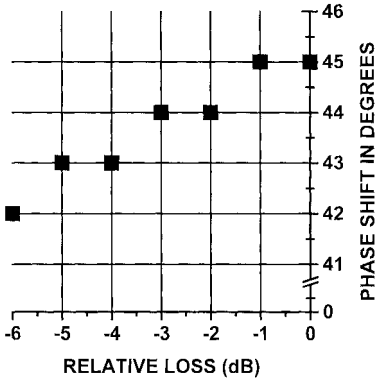

Fig. 10. Measured phase of the reflected wave as a function of the relative insertion loss of the amplitude-phase modulator.

V. Conclusion

A millimeter-wave amplitude-phase modulator, using the polarization principle of phase changing has been successfully designed, fabricated and tested. The fabricated three-bit phase modulator demonstrated accurate phase performance (peak errors were less then 5°), a low level of insertion loss (1 dB), and a low imbalance level (0.3 dB) for the two arbitrarily chosen phase conditions in the 36–37.5-GHz frequency range. The modulator can switch up to 400 mW of RF power with a switching time less than 35 ns, therefore, it is suitable for application in millimeter-wave communication systems. Finally, the possibility of changing the amplitude of the output signal from 0 to −6 dB with an accompanying phase modulation less than 3° was demonstrated.

Acknowledgment

The authors would like to acknowledge the valuable suggestions and helpful discussions received from Dr. V. Skachko,

Dr. Y. Sidoruk, Dr. A. Demchenko, Dr. V. Stashuk, and Dr. P. Stepanenko. The technological support by V. Svirsky, L. Bogdanova, T. Ovdienko, A. Vlasenko, V. Lobasok, C. Espejo, and S. Gonzalez is also appreciated. The authors would also like to thank Dr. N. Bruce for the critical reading of paper, and also gratefully acknowledge the help of Dr. G. Bisiacchi, Dr. C. Firmani, G. Ruiz, J. Sanchez and J-L. Ruiz Llanos.

REFERENCES

[1] H. Meinel, "Commercial applications of millimeter waves history, present status, and future trends," *IEEE Trans. Microwave Theory Tech.*, vol. 43, pp. 1639–1653, July 1995.

[2] F. Ali and J. B. Horton, "Introduction to special issue on emerging commercial and consumer circuits, systems, and their applications," *IEEE Trans. Microwave Theory Tech.*, vol. 43, pp. 1633–1638, July 1995.

[3] K. Feher, "Modulation/microwave integrated digital wireless developments," *IEEE Trans. Microwave Theory Tech.*, vol. 43, pp. 1715–1731, July 1995.

[4] I. Telliez, A. Couturier, and C. Rumelhard, "A compact, monolithic microwave demodulator-modulator for 64-QAM digital radio links," *IEEE Trans. Microwave Theory Tech.*, vol. 39, pp. 1947–1953, Dec. 1991.

[5] H. Callsen, H. Meinel, and W. Hoefer, "P-i-n diode control devices in E-plane technique," *IEEE Trans. Microwave Theory Tech.*, vol. 37, pp. 307–316, Feb. 1989.

[6] H. Phelan, "Spiraphase—A new, low-cost, lightweight phase array. Part 1. Theory and concept," *Microwave J.*, vol. 19, no. 12, pp. 41–44, Dec. 1976.

[7] A. Fox, "An adjustable waveguide phase changer," *PIRE*, vol. 35, no. 12, pp. 1489–1498, Dec. 1947.

Alexander E. Martynyuk was born in Kiev, Ukraine, on June 11, 1965. He received the M. S. degree in radio engineering and the Ph. D. degree from the Kiev Polytechnic Institute (KPI), Kiev, Ukraine, in 1988 and 1993, respectively.

From 1988 to 1995 he was with the Theoretical Radio Engineering Department, KPI. Currently he is a Guest Researcher at the Universidad Nacional Autonoma de Mexico (UNAM), Mexico, in accordance with an agreement between KPI and UNAM. His research interests are in the areas of the millimiter-wave control devices and millimeter-wave communication systems.

Ninel A. Martynyuk was born in Kiev, Ukraine. She received the M. S. degree in radio engineering from the Kiev Polytechnic Institute (KPI), Kiev, Ukraine, in 1994.

In 1996 she was with the Programa Universitario de Investigacion y Desarrollo Espacial, Universidad Nacional Autonoma de Mexico (UNAM), Mexico. She is currently with the Theoretical Radio Engineering Department, KPI. Her research interests include millimeter-wave control devices and FET mixers.

Sergei N. Khotiaintsev (M'94-SM'95) received the M. S. and Ph. D. degrees from Kiev Polytechnic Institute (KPI), Kiev, Ukraine, in 1968 and 1973, respectively.

Beginning in 1973, he worked as a Professor at the KPI, and in 1978 became the Head of the Optical Fiber and Sensor Research Laboratory. He currently works on microwave and laser applications at Puebla University, Puebla, Mexico. He has authored 120 publications and holds 19 patents.

Valeri S. Vountesmeri, photograph and biography not available at time of publication.